TECTONIC AND GRAVITY-FIELD PREDICTIONS FROM EVOLVING CONSTRUCTIONAL MODELS OF LARGE VOLCANOES AND/OR CORONAE ON VENUS. Patrick J. McGovern[1], Alexa K. Schultz[1,2] and Paul K. Byrne[3] [1]Lunar and Planetary Institute (USRA), Houston, TX 77058, [2]Yale University Department of Earth and Planetary Sciences, New Haven, CT 06510, [3]Dept. of Earth, Environmental, and Planetary Sciences, Washington University in St. Louis, St. Louis, MO 63130.

Introduction: The surface of Venus is replete with striking manifestations of volcanic and tectonic activity, including numerous broad shield volcanoes [1, 2] and features with annular topographic and tectonic signatures called coronae [3]. Although the former are attributed to construction via intrusive and extrusive magmatism, the latter are generally interpreted to result from deformation of the lithosphere via uplift and lateral flow of subsurface materials [3].

We have developed quantitative models of evolving volcanic edifice topography [4–6], modulated by lithospheric stress states, to evaluate the conditions that contribute to the wide range of shapes of volcano-tectonic structures on Venus. Some of the topographic shapes generated by such models are annular, as are the orientations of tectonic features predicted by model stress states. Here, we explore the implications of such models for the formation of *a subset* of coronae on Venus, inspired by findings of a "spectrum" of topographic shapes of volcanic landforms that ranges from shield-like to annular, as determined from topographic power spectra [6]. We discuss tectonic and gravity signature predictions based on these models, offering the prospect of evaluating anew formation mechanisms for volcanoes and coronae on Venus with existing and upcoming datasets.

Methods: *Modeling.* We model self-consistent growth of a volcanic edifice on Venus by calculating the interaction of the lithospheric stress state generated by flexure with favored magma ascent pathways [4-7]. The stress state in a lithosphere with elastic thickness T_e is calculated for a given load using the method of [8], using the Hankel Transform integration scheme described in [6] to determine a load function $q(r) = \rho\, g\, h(r)$, where $\rho = 2800$ kg/m^3 is the density of basalt and $g = 8.87$ m/s^2 is the surface gravity of Venus. The load distribution is modeled iteratively: in each model, a characteristic magma source radius (r_0), central height (h_0), and shape (cone, truncated cone, or annulus) are defined [4, 5]. Magma distribution is then subdivided into a number, n_{inc}, of equal height increments. We use $n_{inc} = 1$, 5, 10, or 20; a low n_{inc} value corresponds to a high magma flux rate relative to the characteristic response time of the flexing lithosphere, and vice versa [5]. For a given stress state, magma ascent at a given location is a function of two criteria [4, 5, 7]: favorable horizontal normal stress orientations (i.e., horizontal extension [9]) and gradients (i.e., extension increasing upward [10]). Our model evaluates these criteria as functions of radius r at a discrete set of points, with allowances for favorable stress (e.g., regional) and stress gradient (e.g., magma buoyancy) terms that offset adverse values. Then the magma height for the current increment is assigned to points in r where both ascent criteria are satisfied; at points where one or both criteria are violated, the magma is diverted to the closest value of r where both ascent criteria are satisfied. Next, the material is distributed according to an algorithm [11] simulating lateral motion of flowing lava that enforces downward flow over pre-existing topography and conservation of mass. Then a new flexural stress state is calculated for a load comprising the load from previous increments plus the just-calculated load distribution for the new increment, and the cycle is repeated up to n_{inc} times. The resulting model topographic profiles can be characterized via the same techniques described above for the topographic profiles of actual Venus volcano-tectonic constructs.

Model predictions. We can make predictions of visible patterns of surface tectonics based on the orientations of the dikes that transport magma to the surface according to the two stress-based criteria described above. We can also predict the gravity field resulting from relief on density interfaces via the Hankel-transform approach as follows [12]:

$$\Delta g(k) = 2\,\pi\, G\, e^{-kz}\, \Delta\rho_i\, h_i(k), \qquad (1)$$

where G is the universal gravitational constant, z is elevation above interface, and ρ_i is the density contrast associated with Hankel-transformed relief h_i. If we perform this operation on the surface topography ($\rho_i = \rho_c$) and crust–mantle boundary relief ($\rho_i = \rho_m - \rho_c$) we can sum them to calculate the free-air gravity anomaly.

Results and Discussion: *Tectonics.* For typical corona-shaped constructs (e.g., Fig. 1), there can be fractures with radial or circumferential orientations, or even mixed orientations if both exhibit ascent-favorable stress states. In some locations, flows that spread laterally from other source locations can cover these tectonics structures, as commonly seen at coronae on Venus. In particular, the outer flanks of annular rises and mid-edifice annular lows are likely locations for the burial of previous dike-induced tectonic structures (Fig. 1). We note that source regions may or may not retain the morphological signature of dikes (due to self-coverage by erupted flows and particulars of where vents are circumferentially distributed), but regions where lava accumulates will certainly not retain evidence of such diking. Fig. 2 demonstrates that magma supply rate (through its proxy n_{inc}) affects not

only the topographic profiles but also the visible tectonic states of annular volcanic constructs.

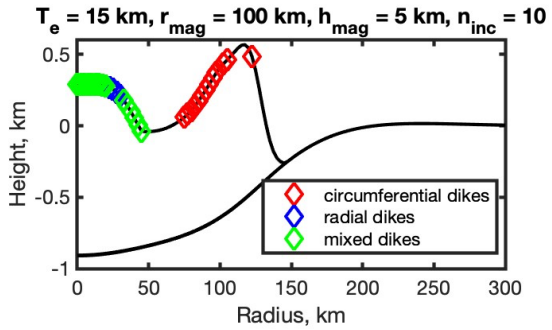

Figure 1. *Topography of edifice and flexural relief for models with* T_e *= 15 km, magma source dimensions* r_{mag} *= 100 km and* h_{mag} *= 5 km, and* n_{inc} *= 10 with superposed orientations of the most recent intrusions that supplied magma to that location, according to the stress criteria outlined above. Locations buried by more than 10 m of lava do not show orientation markers.*

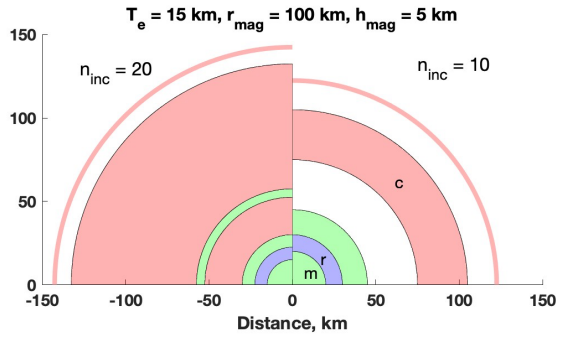

Figure 2. *Map view of tectonic regimes from two models of volcanic corona construction. Light green, blue, and red shades reflect zones of most recent intrusion geometry being mixed, radial, and circumferential dikes, respectively, for models with* n_{inc} *= 20 (left) and* n_{inc} *= 10 (right, as in Fig. 1).*

Gravity. Harmonic analysis of gravity signals from annular loads offers the potential to evaluate the contributions of annular topography and crust–mantle boundary relief to signals contained in current and future gravity datasets. Flexure from an annular edifice load can generate a deflection profile similar to that of a conical edifice for high T_e values (blue lines in Fig. 3), or can give a more "form-fitting" annular profile at low T_e (red lines in Fig. 3). We calculate gravity signals for two limiting wavelengths, corresponding to harmonic degrees 90 and 180: the former represents a substantially above-average value for Magellan gravity degree strength [13], whereas the latter reflects an anticipated global average for VERITAS [14]. Free-air gravity anomaly curves for these two limiting values (Fig. 5b) show that the improvement promised by VERITAS would allow the annular nature of edifices and the flexural responses they generate in the lithosphere to be meaningfully resolved, thereby allowing quantitative tests of corona formation mechanisms.

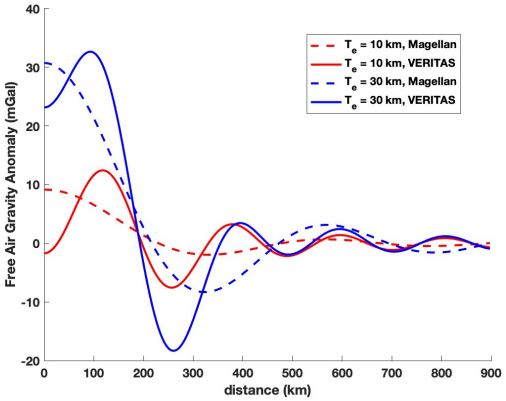

Figure 3. *Free-air gravity anomalies calculated from model density contrast interfaces for annular surface topography with annulus height 1 km and half-radius (distance corresponding to peak height) 100 km, for* T_e *= 10 and 30 km, resolved at wavelengths* λ *= 422 km (high-end Magellan resolution [13]) and* λ *= 211 km (potential VERITAS resolution [14])*

Acknowledgments: This work was supported by NASA SSW grant 80NSSC18K0009, LPI's Cooperative Agreement with NASA, and LPI's Summer Intern Program. We thank Rob Comer for his contributions to establishing the Hankel transform techniques used in this work.

References: [1] Hahn, R. M., & Byrne, P. K. (2023). *JGR: Planets, 128,* e2023JE007753. . [2] L. S. Crumpler et al. (1997) in *Venus II*, U. of Arizona Press, 697-756. [3] E. R. Stofan et al. (1997) in *Venus II*, U. of Arizona Press, 931-965 [4] Buz J. and McGovern P. J. (2010) *LPSC 2010*, abs. 1482. [5] McGovern P. J. and Buz J. (2019) *LPSC 2019*, abs. 2805. [6] Schultz A. and McGovern P. J. (2024) LPSC 2024 (this volume). [7] McGovern P. J. et al. (2013) *JGR: Planets, 118*, 2423–2437. [8] Comer (1983). *Geophys, J. R. astr. Soc., 72,* 101–113. [9] E. M. Anderson (1936) *Proc. R. Soc. Edinburgh, 56*, 128 [10] A. M. Rubin (1995) *Annu. Rev. Earth Planet. Sci., 23*, 287. [11] Webb H. F. and Jordan T. H. (2001) *JGR: Solid Earth, 106*, 30451–30473. [12] R. Comer (1996) personal communication. [13] Konopliv et. al (1999) *Icarus, 139*, 3. [14] Giuliani et al. (2023) DPS 55, abstract 507.06.